

# Optomechanically Induced Sideband Comb

Jun-Hao Liu,<sup>1,2</sup> Guangqiang He,<sup>3</sup> Qin Wu,<sup>4</sup> Ya-Fei Yu,<sup>1</sup> Jin-Dong Wang,<sup>2,\*</sup> and Zhi-Ming Zhang<sup>1,†</sup>

<sup>1</sup>*Guangdong Provincial Key Laboratory of Nanophotonic Functional Materials and Devices  
(School of Information and Optoelectronic Science and Engineering),  
South China Normal University, Guangzhou 510006, China*

<sup>2</sup>*Guangdong Provincial Key Laboratory of Quantum Engineering and Quantum Materials,  
South China Normal University, Guangzhou 510006, China*

<sup>3</sup>*State Key Laboratory of Advanced Optical Communication Systems and Networks,  
Department of Electronic Engineering, Shanghai Jiao Tong University, Shanghai 200240, China*

<sup>4</sup>*School of Biomedical Engineering, Guangdong Medical University, Dongguan 523808, China*

We investigate the nonlinear sideband generation and the induced optical frequency comb (OFC) in a standard cavity optomechanical system (COMS) driven by three laser-fields, including a control field  $\omega_c$  and two probe fields  $\omega_p$  and  $\omega_f$ . The detuning between  $\omega_c$  and  $\omega_p$  ( $\omega_f$ ) is equal to the mechanical frequency  $\omega_b$  ( $\omega_b/n$ ), where  $n$  is a positive integer number, and the intensities of the probe fields are as strong as that of the control field. Due to the optomechanical nonlinearity, the driving energy will be transferred to a series of sidebands, including integer-order, fraction-order, sum and difference sidebands, which constitute an optomechanically induced sideband comb (OMSC). The spectral range and repetition frequency of the OMSC are proportional to the sideband cutoff-order number and interval, respectively. We show that by increasing the intensity of the probe field  $\omega_p$ , we can extend the sideband cutoff-order number and sequentially enlarge the spectral range of OMSC. By increasing the intensity of probe field  $\omega_f$  and decreasing its detuning with control field, we can reduce the sideband interval and consequently decrease the repetition frequency of OMSC. Our work paves the way to achieve the tunable OFC based on COMS.

*Introduction-* Optical frequency comb (OFC) is known as the most accurate “ruler” on the earth [1]. Ever since proposed by Chebotayev [2] and Hänsch [3] in 1970s, it has attracted a lot of attention in many study and application areas, such as ultrafast laser generation [4], tests of fundamental physics with atomic clocks [5], calibration of atomic spectrographs [6], precision time and frequency transfer [7], coherent optical communication [8], molecular fingerprinting [9], precision ranging [10], and so on. The original OFC source is a phase-stabilized mode-locked laser [11], in the time domain the output field of such a mode-locked laser is present as a periodic train of ultrashort pulses, in the frequency domain this pulse train can be transformed as a Fourier series of equidistant optical frequencies. To support more and more broad application space, OFCs have experienced rapid changes over the past 20 years. A lot of new physical systems, such as fiber-based systems [12–14], semiconductor laser platforms [15, 16], microresonator systems [17–20], have been studied for achieving the tunable, miniaturized, and low-powered OFCs. More recently, efforts have also been made in cavity optomechanical system (COMS). An interesting effect named higher-order sideband generation (HSG) is discussed by Xiong et al., and they demonstrate that a tunable higher-order sideband comb can be generated in a ultrastrong driven COMS beyond the perturbative approximation [21, 22].

If we consider an OFC as a “ruler”, the spectral range of the comb will be the length of the “ruler”, and the repetition frequency will be the minimum scale. For an optomechanically induced sideband comb (OMSC), its spectral range is proportional to the sideband cutoff-

order number and its repetition frequency equals to the sideband interval. In previous works, people mainly focus on increasing the sideband cutoff-order number, for example, ones find that many physical effects and systems, such as the Coulomb effect [23], atomic ensemble [24], Casimir effect [25], and the parity-time symmetry structure [26], can effectively increase the cutoff-order number of the higher-order sidebands output from COMS.

Unlike previous works, we are more interested in tuning or decreasing the sideband interval. Actually in the output spectrum of COMS, the sideband interval is equal to the eigenfrequency of the mechanical resonator, and we can decrease the sideband interval by reducing the mechanical frequency. However, owing to the limitation of the processing technology of optomechanical microcavity, it is hard to obtain a microcavity with a small mechanical frequency and a large optomechanical coupling strength. Therefore, ones must explore other ways to decrease the sideband interval. In this letter, we address this problem by driving a standard COMS with three laser-fields which consist of a control field  $\omega_c$  and two probe fields  $\omega_p$  and  $\omega_f$ . We assume that the detuning between  $\omega_c$  and  $\omega_p$  ( $\omega_f$ ) is equal to the mechanical frequency  $\omega_b$  ( $\omega_b/n$ ), in which  $n$  is a positive integer number, and the intensities of the probe fields are as strong as that of the control field. We find that the driving energy will be transferred to a series of nonlinear sidebands, including integer-order, fraction-order, sum and difference sidebands, which constitute an OMSC. We show that the sideband cutoff-order number can be obviously enlarged by increasing the intensity of the probe field  $\omega_p$ , and the sideband interval can be significantly reduced by increasing the intensity of probe field

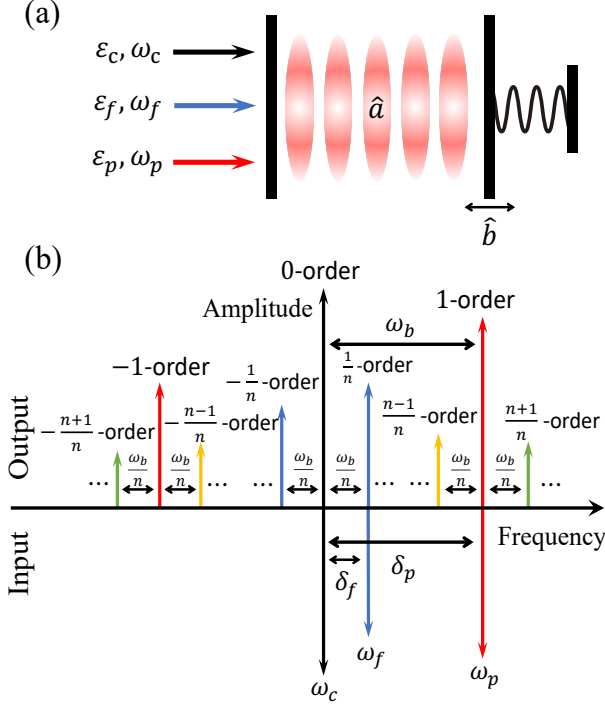


FIG. 1. (color online) (a) Standard optomechanical setup driven by a control field ( $\omega_c$ ) and two probe fields ( $\omega_p, \omega_f$ ). (b) Schematic diagram of the nonlinear sidebands generation. We show the integer-order sidebands (0-order), the fraction-order sidebands ( $\pm \frac{1}{n}$ -order), the sum and difference sidebands ( $\pm \frac{n \pm 1}{n}$ -order).

$\omega_f$  and decreasing its detuning with the control field.

*System model and Hamiltonian*- Our proposed scheme is shown in Fig. 1(a), we consider a standard model of COMS where an optical cavity mode  $\hat{a}$  parametrically couples with a mechanical mode  $\hat{b}$  via radiation pressure. The cavity mode is pumped by three laser-fields  $s_{in}(t) = \epsilon_c e^{-i\omega_c t} + \epsilon_p e^{-i\omega_p t} + \epsilon_f e^{-i\omega_f t}$ , including a control field  $\omega_c$  and two probe fields  $\omega_p$  and  $\omega_f$  with the amplitudes  $\epsilon_y = \sqrt{2\kappa P_y/\hbar\omega_y}$  ( $y = c, p, f$ ), in which  $\kappa$  denotes the cavity damping rate and  $P_y$  refers to the power. The Hamiltonian of the system is given by

$$H = \hbar\omega_a \hat{a}^\dagger \hat{a} + \hbar\omega_b \hat{b}^\dagger \hat{b} + \hbar g \hat{a}^\dagger \hat{a} (\hat{b}^\dagger + \hat{b}) + i\hbar[s_{in}(t)\hat{a}^\dagger + H.c.], \quad (1)$$

where  $\hat{a}$  ( $\hat{a}^\dagger$ ) and  $\hat{b}$  ( $\hat{b}^\dagger$ ) are the bosonic annihilation (creation) operators for the cavity mode and the mechanical mode with frequencies  $\omega_a$  and  $\omega_b$ , respectively.  $g = x_{zpf}\omega_a/L$  is the single-photon optomechanical coupling strength where  $x_{zpf} = \sqrt{\hbar/2M\omega_b}$  is the zero-point uncertainty,  $M$  is the mass of the mechanical oscillator and  $L$  is the rest length of the cavity.

Based on the Hamiltonian (1), the evolution of the system can be described by the Heisenberg-Langevin equa-

tions (in a frame rotating at the frequency  $\omega_c$ ):

$$\dot{\hat{a}} = -(i\Delta_a + \kappa)\hat{a} - ig\hat{a}(\hat{b}^\dagger + \hat{b}) + \epsilon_c + \epsilon_p e^{-i\delta_p t} + \epsilon_f e^{-i\delta_f t} + \sqrt{2\kappa}\hat{a}_{in}, \quad (2)$$

$$\dot{\hat{b}} = -(i\omega_b + \gamma)\hat{b} - ig\hat{a}^\dagger \hat{a} + \sqrt{2\gamma}\hat{b}_{in}, \quad (3)$$

where  $\Delta_a = \omega_a - \omega_c$  is the frequency detuning between the control field  $\omega_c$  and the cavity field  $\omega_a$ .  $\delta_p = \omega_p - \omega_c$  ( $\delta_f = \omega_f - \omega_c$ ) is the frequency detuning between the control field  $\omega_c$  and the probe field  $\omega_p$  ( $\omega_f$ ).  $\gamma$  is the mechanical damping rate.  $\hat{a}_{in}$  and  $\hat{b}_{in}$  are respectively the fluctuation operations corresponding to the cavity mode and the mechanical mode with zero mean value, i.e.,  $\langle \hat{a}_{in} \rangle = \langle \hat{b}_{in} \rangle = 0$ . We focus on the mean response of the system to the probe fields, thus in the following we turn to calculate the evolutions of the expectation values of the system operators  $\hat{a}$  and  $\hat{b}$ , and we denote  $\langle \hat{a} \rangle \equiv \alpha$ ,  $\langle \hat{b} \rangle \equiv \beta$ . By using the mean-field approximation, i.e.,  $\langle \hat{a}\hat{b} \rangle = \langle \hat{a} \rangle \langle \hat{b} \rangle$ , the semiclassical equations of dynamics can be derived from Eqs.(2)-(3) as

$$\dot{\alpha} = -(i\Delta_a + \kappa)\alpha - ig\alpha(\beta + \beta^*) + \epsilon_c + \epsilon_p e^{-i\delta_p t} + \epsilon_f e^{-i\delta_f t}, \quad (4)$$

$$\dot{\beta} = -(i\omega_b + \gamma)\beta - ig|\alpha|^2, \quad (5)$$

we recall that the solutions of the above nonlinear equations have been addressed in previous works for the following three parametric conditions: (i)  $\epsilon_f = 0, \epsilon_p \neq 0, \epsilon_p/\epsilon_c \ll 1$ , under this circumstance the equations can be solved by using the so-called linearization method, and the Stokes and anti-Stokes processes are discussed [27]. (ii)  $\epsilon_f \neq 0, \epsilon_p \neq 0, \epsilon_p/\epsilon_c \ll 1, \epsilon_f/\epsilon_c \ll 1$ , in this case the linearization is practicable, and the sum and difference sidebands effects are investigated [28, 29]. (iii)  $\epsilon_f = 0, \epsilon_p \neq 0, \epsilon_p \sim \epsilon_c$ , in this regime the linearization is inapplicable, by using the numerical calculation, the higher-order sideband effect is studied [21].

In this letter, we study the fourth circumstance, i.e.,  $\epsilon_p \neq 0, \epsilon_f \neq 0, \epsilon_f \sim \epsilon_p \sim \epsilon_c$ , in this regime the expectation value  $x$  ( $x = \alpha, \beta$ ) can be written as

$$x = x_0 + x_p + x_f + x_s + x_d, \quad (6)$$

where  $x_0$  denotes the steady-state solution when  $\epsilon_p = \epsilon_f = 0$ . The optomechanical nonlinearity [corresponding to the terms  $-ig|\alpha|^2$  and  $-ig\alpha(\beta^* + \beta)$ ] will result in the generation of new photons with different frequencies. When the laser-fields are incident upon the cavity, the driving energy will be transferred to the sidebands with a series of new frequencies, which can be expressed as

$$x_p = \sum_{j=1}^N x_{p+}^{(j)} e^{-ij\delta_p t} + x_{p-}^{(j)} e^{ij\delta_p t}, \quad (7)$$

$$x_f = \sum_{k=1}^M x_{f+}^{(k)} e^{-ik\delta_f t} + x_{f-}^{(k)} e^{ik\delta_f t}, \quad (8)$$

similarly to the sum and difference frequency generations in the nonlinear medium, a series of sum and difference sidebands will generate, which are given by

$$x_s = \sum_{j=1}^N \sum_{k=1}^M x_{s+}^{(j,k)} e^{-i(j\delta_p+k\delta_f)t} + x_{s-}^{(j,k)} e^{i(j\delta_p+k\delta_f)t}, \quad (9)$$

$$x_d = \sum_{j=1}^N \sum_{k=1}^M x_{d+}^{(j,k)} e^{-i(j\delta_p-k\delta_f)t} + x_{d-}^{(j,k)} e^{i(j\delta_p-k\delta_f)t}. \quad (10)$$

By solving the governing equation (4)-(5) with the help of the ansatz (6), and using the input-output relation [30]  $S_{out} = S_{in} - \sqrt{2\kappa\alpha} (S_{in} = s_{in} e^{i\omega_c t})$ , we can finally obtain the output spectrum of the system

$$S_{out} = S_0 + S_p + S_f + S_s + S_d, \quad (11)$$

in which we have assumed that the detunings between the probe fields and the control fields satisfy: (i)  $\delta_p = \omega_m$ ; (ii)  $\delta_f = \frac{\omega_m}{n}$  ( $n$  is a positive integer number). It should be noted that the spectrum obtained have shifted the frequency  $\omega_c$ , because Eqs.(4)-(5) describe the evolution of the optical field in a frame rotating at the control frequency. The output spectrum includes the following five parts, as shown in Fig.1(b), the first part  $S_0 = \varepsilon_c - \sqrt{2\kappa\alpha_0}$  is the 0-order sideband which corresponds to the control field  $\omega_c$ . The second and third parts denote the non-zero integer- and fraction-order sidebands, respectively, which can be expressed as

$$S_p = \sum_{j=1}^N A_{p+}^{(j)} e^{-ij\omega_b t} + A_{p-}^{(j)} e^{ij\omega_b t}, \quad (12)$$

$$S_f = \sum_{k=1}^M A_{f+}^{(k)} e^{-i\frac{k}{n}\omega_b t} + A_{f-}^{(k)} e^{i\frac{k}{n}\omega_b t}, \quad (13)$$

we will see a series of sidebands appear at  $\omega = \pm j\omega_b$  and  $\omega = \pm \frac{k}{n}\omega_b$ , in which  $A_{p+}^{(1)}$  and  $A_{f+}^{(1)}$  is called the 1- and  $\frac{1}{n}$ -order sideband, which correspond to the probe field  $\omega_p$  and  $\omega_f$ , respectively. The fourth and fifth parts describe the sum and difference sidebands, respectively, which are given by

$$S_s = \sum_{j=1}^N \sum_{k=1}^M A_{s+}^{(j,k)} e^{-i\frac{jn+k}{n}\omega_b t} + A_{s-}^{(j,k)} e^{i\frac{jn+k}{n}\omega_b t}, \quad (14)$$

$$S_d = \sum_{j=1}^N \sum_{k=1}^M A_{d+}^{(j,k)} e^{-i\frac{jn-k}{n}\omega_b t} + A_{d-}^{(j,k)} e^{i\frac{jn-k}{n}\omega_b t}, \quad (15)$$

that means a series of new sidebands will appear at  $\omega = \pm \frac{jn\pm k}{n}\omega_b$ , and we call  $A_{s\pm}^{(j,k)}$  and  $A_{d\pm}^{(j,k)}$  as the  $\pm \frac{jn+k}{n}$ - and  $\pm \frac{jn-k}{n}$ -order sidebands, respectively.

If all the generated nonlinear sidebands appear in the output spectrum with equal interval, then they will form an optical frequency comb (OFC), and we call it as optomechanically induced sideband comb (OMSC). It can be seen that it is very difficult and tedious to give the

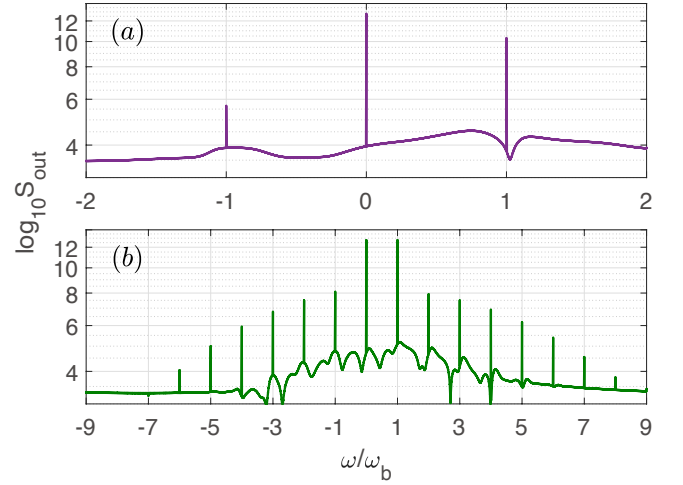


FIG. 2. (color online) The integer-order sidebands spectra for different  $\varepsilon_p$ , (a)  $\varepsilon_p = 9$  GHz, (b)  $\varepsilon_p = 3 \times 10^3$  GHz, the other parameters are stated in the text.

analytical solutions of the sidebands for every orders. To verify our theory and exhibit all the generated sidebands, a more convenient practice is to use the numerical calculation, and we adopt the Runge-Kutta method to solve Eqs.(4)-(5), then the output spectrum can be obtained by using the fast Fourier transform. The used parameters are chosen based on the recent experiment [31] and can be achieved under current technology:  $\omega_b/2\pi = 51.8$  MHz and  $\gamma/2\pi = 41$  kHz (quality factor  $Q_m = 1.26 \times 10^3$ ),  $m = 20$  ng,  $\Delta_a = \omega_b$ ,  $\kappa/2\pi = 15$  MHz,  $g/2\pi = 1$  kHz, the wavelength of the control field  $\lambda_c = 795$  nm, and  $\varepsilon_c = 3 \times 10^3$  GHz.

*Enlarging the spectral range of OMSC-* To exhibit the nonlinear sidebands output from COMS and the generation of OMSC, we firstly assume that  $\varepsilon_f = 0$  and show the integer-order sideband spectra in Fig. 2. We can see that when  $\varepsilon_p$  is weak ( $\varepsilon_p/\varepsilon_c = 3 \times 10^{-2}$ ), there are only 0-order and  $\pm 1$ -order sidebands in the output spectrum. If we increase  $\varepsilon_p$  and when  $\varepsilon_p$  is strong ( $\varepsilon_p/\varepsilon_c = 1$ ), the amplitudes of  $\pm 1$ -order sidebands are strengthened, and the higher integer-order sidebands appear, the positive and negative sidebands end up at the orders of +8 and -6, respectively. Furthermore, for higher order of the sideband, the amplitude is smaller. In general, the sideband cutoff-order number and amplitude both will gradually increase with the increasing of  $\varepsilon_p$ , however the sideband interval does not change and is always  $\omega_b$ . From the point of view of OFC, the integer-order sidebands discussed above constitute an OMSC. By increasing  $\varepsilon_p$ , the spectral range  $f_{sr}$  can be enlarged, for example, the spectral range  $f_{sr} = [-\omega_b, +\omega_b]$  in Fig. 2(a), with the increasing of  $\varepsilon_p$ ,  $f_{sr}$  is enlarged to  $[-6\omega_b, +8\omega_b]$  as Fig. 2(b) shows, whereas the repetition frequency  $f_{rep}$  remains  $\omega_b$ .

*Decreasing the repetition frequency of OMSC-* Below we show the integer-order and fraction-order sideband

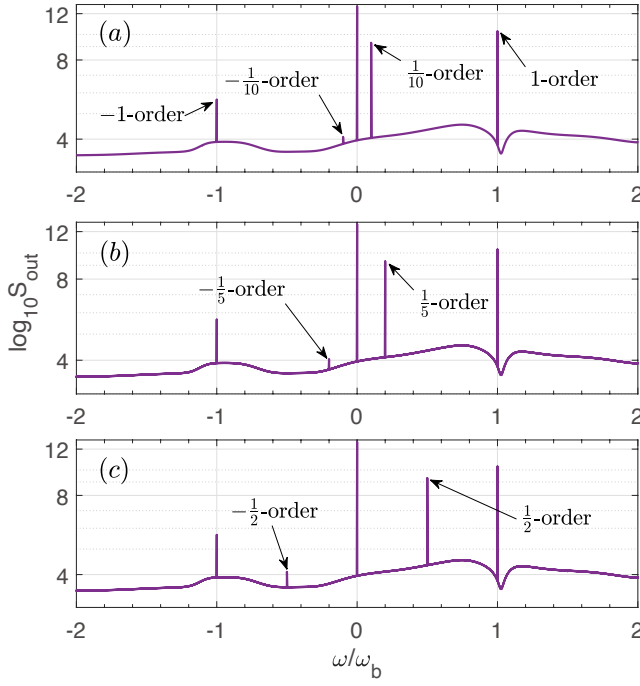


FIG. 3. (color online) The integer-order and fraction-order sidebands spectra for different  $n$ , (a)  $n = 10$ , (b)  $n = 5$ , (c)  $n = 2$ .  $\varepsilon_f = 9 \times 10^{-1}$  GHz, and the other parameters are the same as that in Fig. 2(a).

spectra for different  $n$ , as shown in Fig. 3, we consider another probe field  $\omega_f$  is inputted into the cavity with a very small amplitude ( $\varepsilon_f/\varepsilon_c = 3 \times 10^{-3}$ ), and the other conditions are the same as that in Fig. 2(a). It can be seen that the integer-order sidebands have hardly changed, while two new fraction-order sidebands appear, and their positions depend on  $n$ . Especially when  $n = 2$ , the new generated  $\pm \frac{1}{2}$ -order sidebands and the pre-existing 0-order and  $\pm 1$ -order sidebands constitute an OMSC with a smaller repetition frequency  $f_{rep} = \omega_b/2$ . However, the spectral range  $f_{sr}$  remains  $[-\omega_b, \omega_b]$ .

Figure 4 displays the higher integer-order, fraction-order, sum and difference sidebands spectra for different  $\varepsilon_f$ , and the other conditions are the same as that in Fig. 2(b). When  $\varepsilon_f/\varepsilon_c = 3 \times 10^{-2}$ , the amplitudes of  $\pm \frac{1}{10}$ -order sidebands are obviously enhanced compared with that in Fig. 3(a), and the sum and difference sidebands between  $\pm \frac{1}{10}$ -order and the integer-order sidebands, such as  $\pm \frac{11}{10}$ -order,  $\pm \frac{9}{10}$ -order,  $\pm \frac{19}{10}$ -order,  $\pm \frac{21}{10}$ -order sidebands, etc., can be seen in the output spectrum. Furthermore, the higher fraction-order sidebands, such as  $\pm \frac{2}{10}$ -order sidebands come out, and the sum and difference sidebands between  $\pm \frac{2}{10}$ -order and the integer-order sidebands can be also seen, for example,  $\pm \frac{18}{10}$ -order,  $-\frac{22}{10}$ -order sidebands, and so on. When  $\varepsilon_f/\varepsilon_c = 2 \times 10^{-1}$ , there are more higher fraction-order sidebands, such as  $\pm \frac{4}{10}$ -order sidebands, and more sum and difference sidebands, such as  $-\frac{26}{10}$ -order,  $\frac{46}{10}$ -order

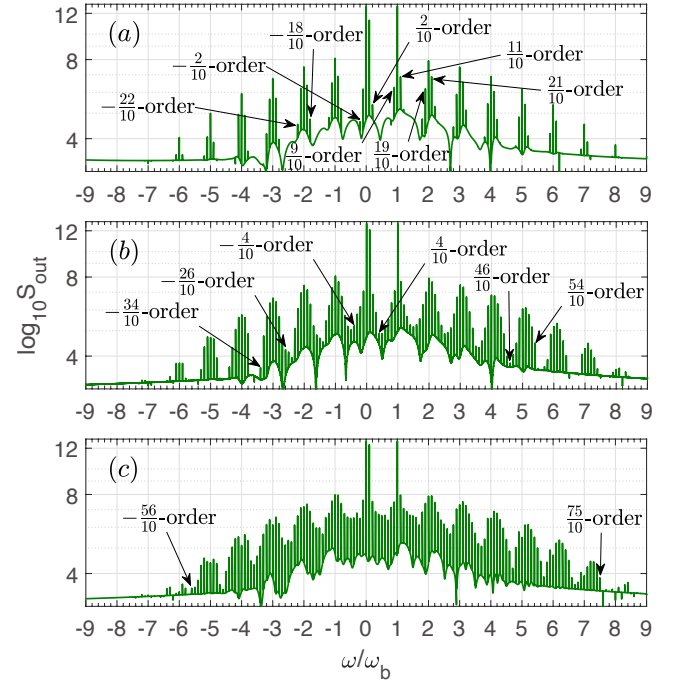


FIG. 4. (color online) The higher integer-order, fraction-order, sum, and difference sidebands spectra for different  $\varepsilon_f$ , (a)  $\varepsilon_f = 9 \times 10^1$  GHz, (b)  $\varepsilon_f = 6 \times 10^2$  GHz, (c)  $\varepsilon_f = 1.2 \times 10^3$  GHz.  $n = 10$ , and the other parameters are the same as that in Fig. 2(b).

sidebands. The all generated nonlinear sidebands (from  $-\frac{34}{10}$ -order to  $\frac{54}{10}$ -order) come into being an OMSC with the spectral range  $f_{sr} = [-\frac{34}{10}\omega_b, +\frac{54}{10}\omega_b]$  and repetition frequency  $f_{rep} = \omega_b/10$ . If we continue to increase  $\varepsilon_f$  and when  $\varepsilon_f/\varepsilon_c = 4 \times 10^{-1}$ , we can see that more sum and difference sidebands appear, for example,  $-\frac{56}{10}$ -order,  $\frac{75}{10}$ -order sidebands, from the angle of OMSC, now  $f_{sr}$  approximately equals to that in Fig. 2(b) while  $f_{rep}$  is decreased by one order of magnitude.

*Conclusions-* In summary, we have shown the optomechanical induced nonlinear sideband generation in a standard optomechanical system driven by three strong laser fields, the output sidebands with equal interval will come into being an OMSC. We show that the sidebands cutoff-order number can be extended by increasing the intensity of the probe field  $\omega_p$ , which results in the enlargement of the spectral range of OMSC. In addition, the sidebands interval can be reduced by increasing the intensity of the probe field  $\omega_f$  and decreasing its detuning with the control field, which leads to the diminution of the repetition frequency of OMSC. We conclude that the challenge to achieve the tunable OFC based on COMS will be greatly aided by our work.

This work was supported by the National Natural Science Foundation of China (Grant Nos. 61941501, 61775062, 11574092, 61378012, and 91121023), Doctoral Program of Guangdong Natural Science Foundation

(No.2018A030310109), Doctoral Project of Guangdong Medical University (No.B2017019), and Open Project of the Key Laboratory of Low Dimensional Quantum Structures and Quantum Control of the Ministry of Education, Hunan Normal University (No. QSQC1808).

---

\* wangjingdong@m.scnu.edu.cn

† zhangzhiming@m.scnu.edu.cn

- [1] T. Fortier and E. Baumann, *Commun. Phys.* **2**, 1 (2019).
- [2] Y. V. Baklanov and V. P. Chebotayev, *Appl. Phys. A* **12**, 97 (1977).
- [3] J. N. Eckstein, A. I. Ferguson, and T. W. Hänsch, *Phys. Rev. Lett.* **40**, 847 (1978).
- [4] U. Keller, *Nature* **424**, 831 (2003).
- [5] T. Rosenband, D. B. Hume, P. O. Schmidt, C. W. Chou, A. Brusch, L. Lorini, et al., *Science* **319**, 1808 (2008).
- [6] M. T. Murphy, T. Udem, R. Holzwarth, A. Sismann, L. Pasquini, C. Araujo-Hauck, et al., *Mon. Not. R. Astron. Soc.* **380**, 839 (2007).
- [7] F. R. Giorgetta, W. C. Swann, L. C. Sinclair, E. Baumann, I. Coddington, and N. R. Newbury, *Nat. Photon.* **7**, 434 (2013).
- [8] P. Marin-Palomo, J. N. Kemal, M. Karpov, A. Kordts, J. Pfeifle, M. H. P. Pfeiffer, et al., *Nature*, **546**, 274 (2017).
- [9] S. A. Diddams, L. Hollberg, and V. Mbele, *Nature* **445**, 627 (2007).
- [10] K. Minoshima and H. Matsumoto, *Appl. Opt.* **39**, 5512 (2000).
- [11] T. M. Fortier, P. A. Roos, D. J. Jones, S. T. Cundiff, R. D. R. Bhat, and J. E. Sipe, *Phys. Rev. Lett.* **92**, 147403 (2004).
- [12] S. Schilt and T. Sdmeyer, *Appl. Sci.* **5**, 787 (2015).
- [13] W. Xia and X. Chen, *Meas. Sci. Technol.* **27**, 041001 (2016).
- [14] S. Duval, M. Bernier, V. Fortin, J. Genest, M. Pich, and R. Valle, *Optica* **2**, 623 (2015).
- [15] S. M. Link, A. Klenner, M. Mangold, C. A. Zaugg, M. Golling, B. W. Tilma, and U. Keller, *Opt. Express* **23**, 5521 (2015).
- [16] L. A. Sterczewski, J. Westberg, Y. Yang, D. Burghoff, J. Reno, Q. Hu, and G. Wysocki, *Optica* **6**, 766 (2019).
- [17] P. DelHaye, A. Schliesser, O. Arcizet, T. Wilken, R. Holzwarth, and T. J. Kippenberg, *Nature* **450**, 1214 (2007).
- [18] A. A. Savchenkov, A. B. Matsko, V. S. Ilchenko, I. Solomatine, D. Seidel, and L. Maleki, *Phys. Rev. Lett.* **101**, 093902 (2008).
- [19] V. Brasch, E. Lucas, J. D. Jost, M. Geiselmann, and T. J. Kippenberg, *Light-Sci. Appl.* **6**, e16202 (2017).
- [20] T. Herr, V. Brasch, J. D. Jost, C. Y. Wang, N. M. Kondratiev, M. L. Gorodetsky, and T. J. Kippenberg, *Nat. Photon.* **8**, 145 (2014).
- [21] H. Xiong, L. G. Si, X. Y. L, X. X. Yang, and Y. Wu, *Opt. Lett.* **38**, 353 (2013).
- [22] H. Xiong, L. G. Si, X. Y. L, X. X. Yang, and Y. Wu, *Ann. Phys-New York* **349**, 43 (2014).
- [23] K. Cui, H. Xiong, and Y. Wu, *Phys. Rev. A* **95**, 033820 (2017).
- [24] Z. X. Liu, H. Xiong, and Y. Wu, *Phys. Rev. A* **97**, 013801 (2018).
- [25] J. Yao, Y. F. Yu, and Z. M. Zhang, *Chin. Opt. Lett.* **16**, 111201(2018).
- [26] L. Y. He, *Phys. Rev. A* **99**, 033843 (2019).
- [27] S. Huang and G. S. Agarwal, *Phys. Rev. A* **81**, 033830 (2010).
- [28] H. Xiong, Y. W. Fan, X. X. Yang, and Y. Wu, *Appl. Phys. Lett.* **109**, 061108 (2016).
- [29] H. Xiong, Z. X. Liu, and Y. Wu, *Opt. Lett.* **42**, 18 (2017).
- [30] C. W. Gardiner and M. J. Collett, *Phys. Rev. A* **31**, 3761 (1985).
- [31] S. Weis, R. Rivière, S. Deléglise, E. Gavartin, O. Arcizet, A. Schliesser, and T. J. Kippenberg, *Science* **330**, 1520 (2010).